

LASER APPLICATIONS AND OTHER TOPICS IN QUANTUM ELECTRONICS https://doi.org/10.1070/QEL17189

Nanodiamonds with SiV colour centres for quantum technologies

A.I. Zeleneev, S.V. Bolshedvorskii, V.V. Soshenko, O.R. Rubinas,
A.S. Garanina, S.G. Lyapin, V.N. Agafonov, R.E. Uzbekov, O.S. Kudryavtsev,
V.N. Sorokin, A.N. Smolyaninov, V.A. Davydov, A.V. Akimov

Abstract. **Properties of silicon-vacancy (SiV) colour centres in ultra-nanosize diamonds are studied. Nanodiamonds are obtained at a high temperature and pressure, which induced transformations in mixtures of organic and hetero-organic compounds without metal-catalysts. The size distribution of grown nanodiamonds is determined by the methods of transmission electron microscopy and atomic-force microscopy, as well as by using the model of phonon spatial localisation. In addition, Raman spectra of various nanodiamonds and luminescence properties of SiV-centres are investigated.**

A.I. Zeleneev Moscow Institute of Physics and Technology (State University), Institutskii per. 9, 141701 Dolgoprudnyi, Moscow region, Russia; Russian Quantum Centre, Bol'shoi bul'var 30, stroenie 1, Skolkovo, 121205 Moscow, Russia; Photonic Nano-Meta Technologies, ul. Nobelya, 7, Skolkovo, 143026 Moscow, Russia; e-mail: zeleneev.ai@phystech.edu;
S.V. Bolshedvorskii Moscow Institute of Physics and Technology (State University), Institutskii per. 9, 141701 Dolgoprudnyi, Moscow region, Russia; Lebedev Physical Institute, Russian Academy of Sciences, Leninsky prosp. 53, 119991 Moscow, Russia; Photonic Nano-Meta Technologies, ul. Nobelya, 7, Skolkovo, 143026 Moscow, Russia;
V.V. Soshenko Lebedev Physical Institute, Russian Academy of Sciences, Leninsky prosp. 53, 119991 Moscow, Russia; Photonic Nano-Meta Technologies, ul. Nobelya, 7, Skolkovo, 143026 Moscow, Russia;
O.R. Rubinas Moscow Institute of Physics and Technology (State University), Institutskii per. 9, 141701 Dolgoprudnyi, Moscow region, Russia; Russian Quantum Centre, Bol'shoi bul'var 30, stroenie 1, Skolkovo, 121205 Moscow, Russia; Lebedev Physical Institute, Russian Academy of Sciences, Leninsky prosp. 53, 119991 Moscow, Russia; Photonic Nano-Meta Technologies, ul. Nobelya, 7, Skolkovo, 143026 Moscow, Russia;
A.S. Garanina, V.N. Agafonov, R.E. Uzbekov. University of Tours, 60 Rue du Plat d'Étain, Tours, 37032, France;
S.G. Lyapin, V.A. Davydov Vereshchagin Institute for High Pressure Physics, Russian Academy of Sciences, Kaluzhskoe sh. 14, Troitsk, 108840 Moscow, Russia;
O.S. Kudryavtsev Prokhorov General Physics Institute, Russian Academy of Sciences, ul. Vavilova 38, 119991 Moscow, Russia;
V.N. Sorokin Russian Quantum Centre, Bol'shoi bul'var 30, stroenie 1, Skolkovo, 121205 Moscow, Russia; Lebedev Physical Institute, Russian Academy of Sciences, Leninsky prosp. 53, 119991 Moscow, Russia;
A.N. Smolyaninov Photonic Nano-Meta Technologies, ul. Nobelya, 7, Skolkovo, 143026 Moscow, Russia;
A.V. Akimov Russian Quantum Centre, Bol'shoi bul'var 30, stroenie 1, Skolkovo, 121205 Moscow, Russia; Lebedev Physical Institute, Russian Academy of Sciences, Leninsky prosp. 53, 119991 Moscow, Russia; Texas A&M University, College Station, TX 77843, USA

Received 14 November 2019, revised 19 December 2019
Kvantovaya Elektronika **50** (3) 299–304 (2020)
Translated by N.A. Raspopov

Keywords: *nanodiamonds, SiV colour centre, stresses in a crystal lattice, Raman spectroscopy, luminescence spectroscopy, probe microscopy.*

1. Introduction

The development of methods for synthesising fluorescent diamonds with prescribed properties, in particular, ultra-nanosize (~10 nm and less) diamonds, is an actual problem of modern materials science due to the employment of such materials in new biomedical [1, 2] and quantum-physics [3, 4] applications.

There are several ways to synthesise nanodiamonds of size less than 10 nm. One method is the shock-blast synthesis, which provides obtaining detonation nanodiamonds with classical sizes (5 ± 2 nm) [5]. However, nanodiamonds obtained in this way exhibit tendency to aggregation; thus, separation of single nanodiamonds becomes a challenging task. A detonation nanodiamond is characterised by a complicated crystal structure, which is related to the process of its origin [6, 7]. Such a nanoparticle is a diamond nucleus with various crystal lattice defects (admixtures, dislocations, colour centres), surrounded by a transient layer of graphitised carbon in the sp^2- and sp^3-states and a surface envelope, which includes various types of functional groups. Consequently, this method of synthesis cannot produce nanodiamonds (with a size of less than 10 nm) with a definite structure. One more method for producing nanodiamonds of size less than 3–4 nm, namely, chemical deposition from gas phase [8], has a high level of internal stresses, which is a serious drawback.

An alternate method for obtaining nanodiamonds is the synthesis of macro-size diamonds (followed by mechanical grinding) and nanosize diamonds (with the addition of boron-containing compound 9BBN [9], adamantine [10], and other components) at high pressures and temperatures. Its main advantage over the shock-blast method is that the diamond material obtained in this way has a high-quality homogeneous crystal structure, which is rather important in sensor and quantum applications of nanodiamonds [11, 12].

It is known that sensor and quantum applications utilise colour centres that are the point defects of a diamond crystal lattice, which arise when such centres replace carbon atom in a lattice site and bind to vacancies in neighbouring sites. The most interesting colour centres in diamond are nitrogen-vacancy (NV centre) [13], nickel centre (NE8) [14], nickel-silica complex [14], germanium-vacancy (GeV centre) [15], chromium colour centres [16], tin-vacancy (SnV centre) [17], and silica-vacancy (SiV centre) [18]. Each of the studied kinds of colour centres is applied in various fields. Therefore, the most

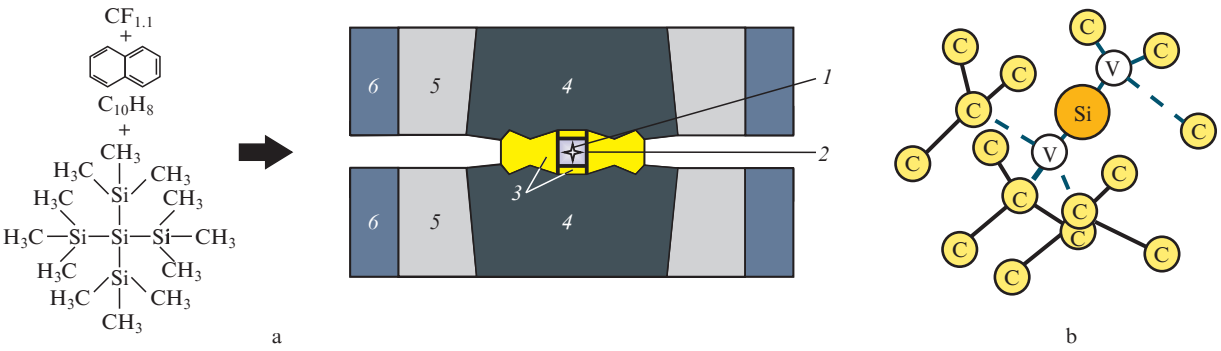

Figure 1. (a) Schematic of a high-pressure chamber for obtaining nanodiamonds comprising SiV centres and (b) crystal structure of a SiV centre in diamond:
(*1*) reaction zone; (*2*) graphite heater; (*3*) catlinite container and catlinite heat-insulating disks; (*4*) tungsten carbide anvil; (*5*, *6*) steel holding rings.

studied NV centre makes it possible to realise optical reading and long-term coherence of an electron spin state [19]; however, its phononless line is weak with the integral intensity equal to 2%–3% of the emission spectrum integral intensity. Later, an alternative to NV-centre was suggested in the form of SiV centres [20, 21], which photoluminescence is concentrated (70%) [22] in a narrow (with a width of ~5 nm) and intensive phononless line [23, 24].

A SiV centre comprises one silica atom surrounded by six carbon atoms at equal distances from it. The silica atom replaces two carbon atoms in the diamond lattice cell and may occupy one of the 16 crystallographic positions with D_{3d} symmetry, which may be disposed on one of the axes of [111] type (Fig. 1b).

The present work is aimed at studying the possibility of producing ultranano- (~10 nm) and nanosize (10–100 nm) fluorescing diamonds with the impurity-vacancy SiV centres by transforming mixtures of hydrocarbon and hetero-organic compounds free of traditional metal-catalysts under a high pressure and temperature. In addition, optical properties, the degree of crystal perfection, and level of internal stresses of the obtained fluorescent diamonds have also been investigated.

2. Synthesis of nanodiamonds

Nanodiamonds have been synthesised by thermobaric treatment of homogeneous mixtures comprised of naphthalene $C_{10}H_8$ (Chemapol), high-fluorine graphite $CF_{1.1}$ (Aldrich Chemical) and tetrakis(trimethylsilyl)silane $C_{12}H_{36}Si_5$ (Stream Chemicals) [25, 26] with the employment of a high-pressure device of Toroid type (Fig. 1). In this case, fluorinated graphite play the role of a fluorinate component in the initial mixture, which reduces *p*- and *T*-parameters of diamond formation in a hydrocarbon system and favours increasing the fraction content of ultranano- and nanosize diamonds during the transformation [27]. Tetrakis(trimethylsilyl)silane served as a siliceous dopant component in the growing system. Compacted tablets of the initial mixture (with a diameter of 5 mm and height of 3 mm) were placed into a graphite container that also served as a high-pressure heating device.

Diamond synthesis was performed at a pressure of 8 GPa, temperature 11100–1400 °C and short (1–5 s) isothermal exposure times. After cooling and unloading, the samples produced were withdrawn from the high-pressure unit and investigated at normal conditions by X-ray diffraction, Raman spectroscopy, scanning (SEM) and transmission (TEM) electron microscopy.

According to the data of sample preliminary certification, diamond is the main transformation product in initial growing systems. The samples may comprise impurities in the form of negligible (1%–5%) quantities of graphite and amorphous carbon as well as intermediate transformation products not converted to diamond. Note that the fraction composition of diamond products, that is, relative contents of ultranano-, nano-, submicro- (100–1000 nm), and micro-size (above 1000 nm) diamonds substantially depends on the initial growing mixture composition, temperature, and duration of the isothermic exposure. Since the work is aimed at obtaining and studying the smallest fluorescent diamonds, the synthesis mainly included the fluorinating component at temperatures close to the diamond production temperature threshold and minimal isothermic exposure duration, which limited collective recrystallisation of produced particles of ultranano- and nanosize diamonds.

All the conditions mentioned favour increasing the content of finest diamond fractions in synthesis products. Note also that there is a radial temperature gradient in the reaction zone of the high-temperature unit with a cylindrical heater. Hence, the temperature at the reaction zone centre is lower than in the zone near heater walls, and the finest diamond fractions are obtained, as a rule, at the reaction zone centre. Greater fractions are produced in the zone where the reaction mixture is close to the heater walls.

Non-diamond carbon impurities were removed from synthesised samples in the process of boiling in a 40%-solution of hydrogen peroxide. Ultrasound dispersion of diamond nanoparticles in water medium was performed by an ultrasound disperser UP200Ht (Hielscher Ultrasonic Technology) at a power of 200 W for an hour. The aqueous dispersions obtained were then employed for separating diamond product fractions by size in stepwise centrifuging of aqueous diamond dispersions at various overload values (1000*g*, 3000*g*, and 5000*g*). Then, the diamond fraction with smallest dimensions residual in the suspension state after centrifuging at 5000*g* was investigated.

3. Study of nanodiamond size distribution

A TEM-image of a separated diamond fraction is presented in Fig. 2a. One can see that majority of separated nanodiamonds had the size not greater than 20 nm. A histogram of

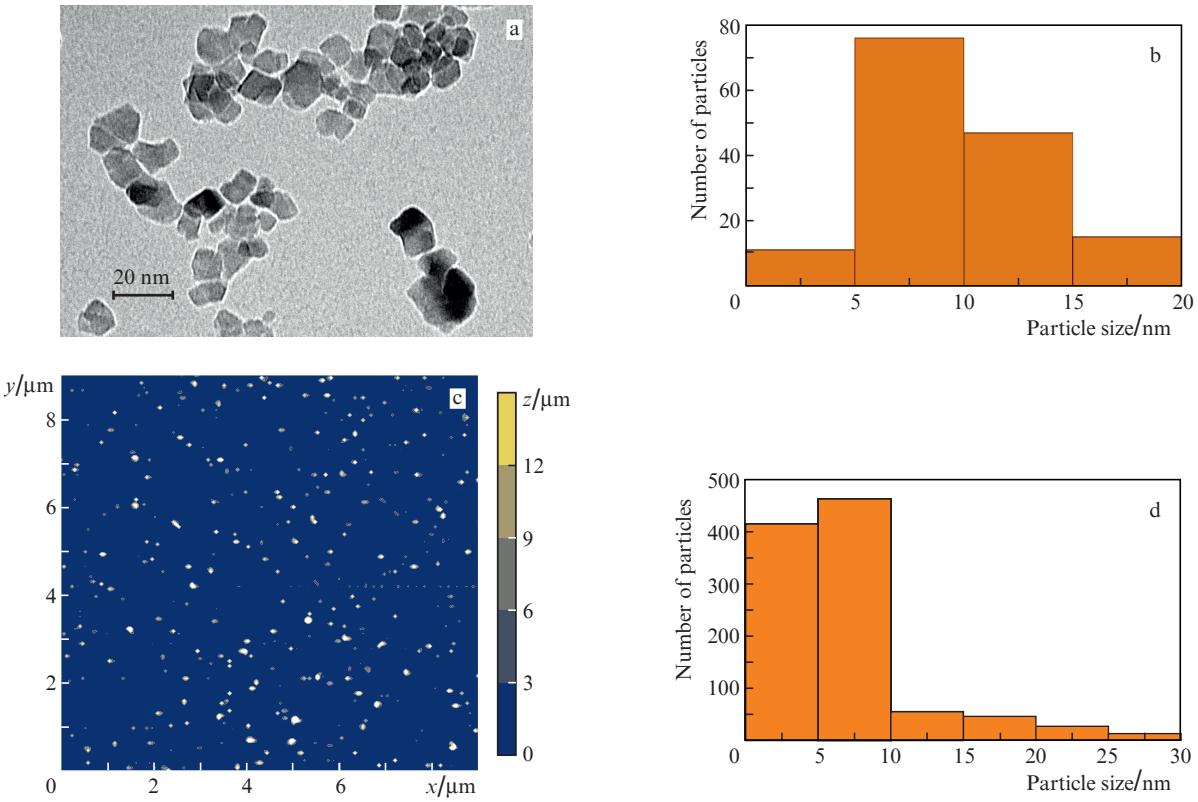

Figure 2. (Colour online) (a) TEM-image of nanoparticles of separated diamond fraction, (b) histogram of nanoparticle size distribution based on the results of analysis of TEM-images comprising 149 nanoparticles, (c) AFM-map with investigated nanodiamonds on a glass substrate and (d) histogram of the size distribution of the synthesised nanodiamonds which dimensions have been determined by analysing the AFM-maps comprising 1019 nanodiamonds.

the statistical analysis performed for four TEM-images based on 149 measured particles is shown in Fig. 2b. One can see that the median size of the selected diamond group is 7.5 ± 5 nm.

We have additionally determined the nanodiamond size by the method of atomic force microscopy (AFM), which provides a more complete statistics of particle size distribution for nanoparticles smaller than 5 nm. AFM-maps have been obtained by using a NTEGRA Spectra-M (NT-MDT) microscope with a silica cantilever HA_NC (NT-MDT) operated in a contact-free mode. For analysis, nanodiamonds were deposited onto a glass substrate (Menzel Gläser) through evaporation from a colloid solution in vacuum [28]. Totally, three AFM-maps have been studied (a typical map is presented in Fig. 2c), which comprised 1019 nanodiamonds and their small aggregates. From these maps, the histogram of nanodiamonds size distribution was plotted with a median value of 5.5 ± 5 nm, which agrees with the results of TEM analysis (Fig. 2b). However, a higher resolution of the AFM method yields a greater number of particles with the size of less than 5 nm, as compared to the TEM method.

4. Study of nanodiamond crystal lattice

The diamond material quality was initially estimated by using the high-resolution TEM method (Fig. 3a). One can see that the nanodiamond in the figure has a high quality, which is confirmed by the absolute periodicity of its crystal structure, lacking edge and screw dislocations, and observed faceting. The crystal lattice of the grown diamond material was more accurately analysed by performing X-ray diffraction (XRD) study of dried diamond suspension. Results of the analysis are given in Fig. 3b. The diffraction peak profile obtained is well approximated by the Lorentz function near the diamond diffraction angle with the crystallographic orientation [111]. The diffraction peak of synthesised diamonds is observed at the angle $2\theta = 43.85° \pm 0.01°$ and has the width $\gamma = 0.90° \pm 0.01°$. The diffraction peak of synthesised nanodiamonds is symmetrical, and its maximum is slightly shifted relative to that of a single-crystal nanodiamond with orientation [111] ($2\theta = 43.91°$) [29], which is typical for nanodiamonds [29]. Issuing from the results obtained we may conclude that the crystal structure of synthesised nanodiamonds is almost perfect.

Raman spectra were recorded by using a TriVista 555 spectrometer (Princeton Instruments) with an Olympus BX51 objective at magnification of 50×. Radiation of an Ar^+-laser at a wavelength of 488 nm was used for excitation. Raman spectra of the synthesised nanodiamonds prior to their purification and centrifuging are given in Figs 3c and 3e, and after these procedures in Figs 3d and 3f. Disappearance of the broad wings in Raman spectra after the purification of 'raw' diamond material indicates that some carbon non-diamond forms are comprised in the initial diamond material. After purification, only two specific peaks are revealed in the spectrum: the diamond peak at a frequency of 1330 cm^{-1} and graphite-like carbon peak at the frequency of 1590 cm^{-1}, which corresponds to the G-band related with plane vibrations of carbon atoms in graphite [29]. By the frequency difference between these peaks, one can judge the purity of a

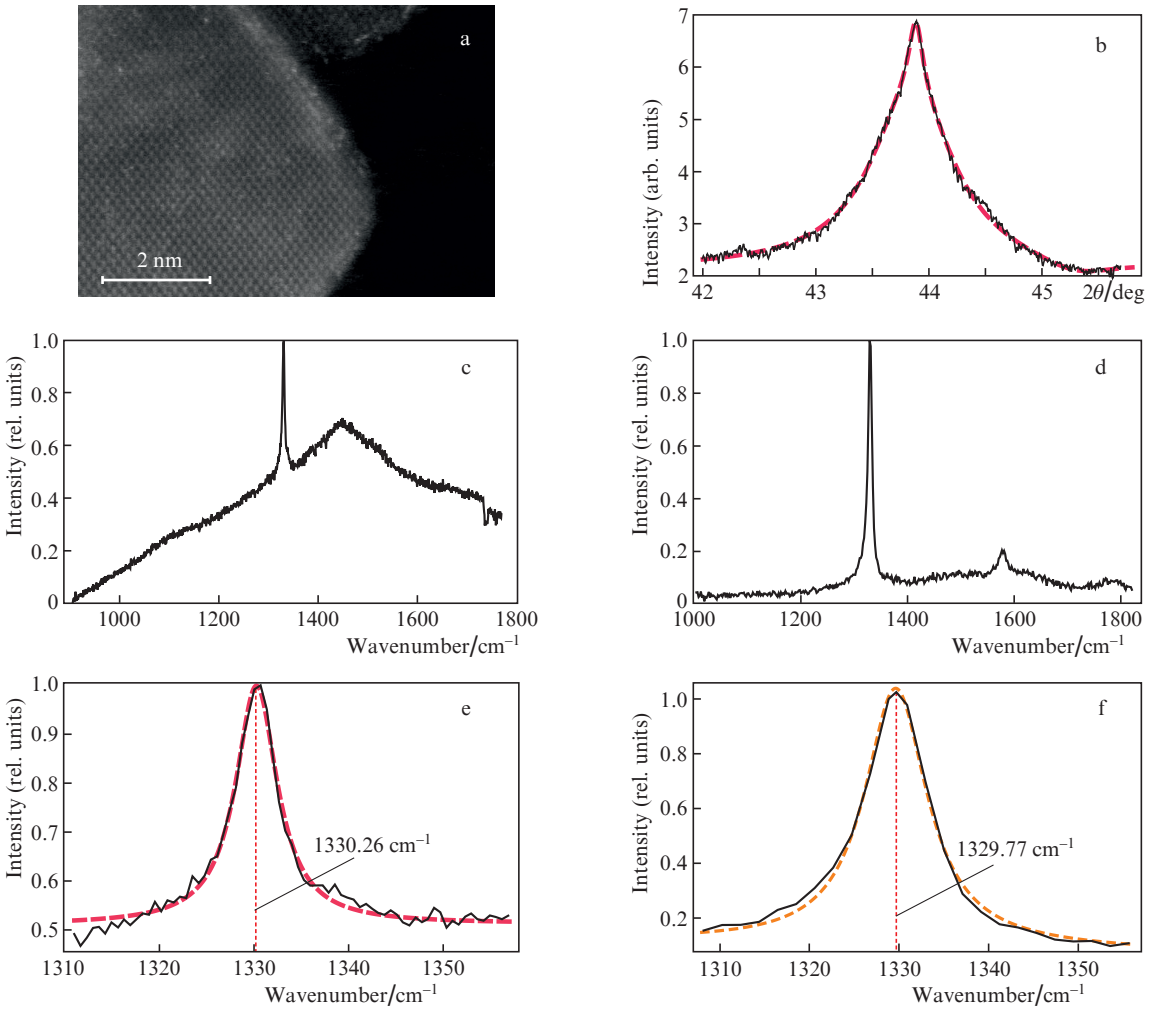

Figure 3. (a) High-resolution TEM-image of a single nanodiamond, (b) X-ray diffraction peak along the [111] axis of synthesised diamond material, approximated by the Lorentz function (dashed curve), (c, d) Raman spectra of the diamond material obtained (c) immediately after the growing prior to purification and centrifuging and (d) after those, and (e, f) peaks of Raman spectra of diamond obtained (e) immediately after the growing prior to the purification and centrifuging processes and (f) after those. The peak profiles (e, f) are approximated by the Lorentz function (dashed curves); vertical lines indicate positions of the peak centres, determined from approximation.

final diamond material: in our case, one can see that diamond carbon in the sp^3-state prevails over other carbon fractions. Consider the diamond peak in more details, because its position gives information about quality of the crystal structure, and it is possible to estimate an average dimension of synthesised diamonds basing on the phonon spatial localisation theory.

Figures 3e and 3f show Raman peaks of the diamond material obtained after the growing prior to purification and centrifuging procedures and after those, respectively. We have approximated these peaks by Lorentz function and determined in this way the positions of Raman lines for diamond:$\nu_1 = 1330.26 \pm 0.35$ cm^{-1} at the FWHM line width $\Gamma_1 = 5.3 \pm 0.6$ cm^{-1} for diamond material prior to purification and centrifuging procedures. For diamond material after purification and centrifuging procedures, we obtained $\nu_2 = 1329.77 \pm 0.35$ cm^{-1} at the FWHM line width $\Gamma_2 = 8.45 \pm 0.7$ cm^{-1}. For synthesised diamonds, the peak of the Raman line is broadened and its position is slightly shifted left relative to that of a single-crystal diamond at the frequency $\nu_0 = 1331.8$ cm^{-1}. This effect can be explained by internal stresses and defects of crystal lattice, as well as by spatial localisation of phonons. In view of a high quality of the crystal structure (Fig. 2a) we assume that the main contribution is made by spatial localisation of phonons related to small crystal dimensions [29–31].

From a Raman spectrum, one can estimate dimensions of synthesised diamonds basing on the theory of phonon spatial localisation [31, 32]. For the fraction of ultra-nanosize diamonds obtained after purification and centrifuging procedures, the characteristic dimension L is 9 ± 1 nm. Within the error limits, this result coincides with the nanodiamond size found from direct measurements. This confirms that the width and shift of Raman line peak in diamond is mainly affected by spatial localisation of phonons.

Thus, issuing from the Raman spectrum, which characterises the diamond carbon hybridisation form sp^3 one can assert that synthesised nanodiamond have the size of less than 10 nm and a high-quality crystal lattice.

5. Fluorescent properties of nanodiamonds

One of the characteristics determining the quality of synthesised nanodiamonds is luminescence of their colour centres.

We have studied luminescence spectra of SiV-centres comprised in nanodiamonds. All the spectral measurements were taken at room temperature by using a self-made spectrometer, comprised of a monochromator 82-422 (Jarrel Ash) and CCD-camera SXV-H9C (Starlight Xpress). Totally, 44 spectra have been recorded for SiV centres in various nanodiamonds, each of them comprising from one to ten SiV centres. The spectral sensitivity of the device has been taken into account in all spectral measurements. Each spectrum (Figs 4a, 4b) was approximated by a sum of three Lorentz functions [33], from which two functions are responsible for phonon wings and one function corresponds to a phononless line.

Histograms in Fig. 4c characterise the dispersion of a phononless line centre position, and Fig. 4d presents the FWHM width Γ for each line from the spectra. It was found that an average value of a phononless line centre position corresponds to the wavelength of 738.06 ± 0.27 nm, and the width Γ of the line at room temperature is 5.9 ± 0.8 nm. The second result is classical for room temperature because it is mainly determined by a strong coupling of SiV-centre electrons in excited states with phonons of diamond crystal lattice [34, 35], whereas the narrow spread of phononless line centre position points to the low internal stresses in nanodiamond crystal lattice, which mainly determine the spread [36]. We can estimate the upper limit for internal stresses of the crystal lattice by using the dispersion of a phononless line position from the histogram: $\sigma = 0.27$ nm. For this purpose, we will employ the classical dependence of phononless line energy E on an external pressure p:

$$E(p) = E_0 + \alpha p + \beta p^2,$$

where $E_0 = 1.68$ eV, $\alpha = 1.09$ meV GPa^{-1}, and $\beta = -5.7 \times 10^{-3}$ meV GPa^{-2} are the coefficients obtained experimentally [36]. In view of $\alpha \gg \beta$ we may limit ourselves to linear approximation. Then, by using the recalculated value $\alpha = 0.48$ nm GPa^{-1}, the upper limit of internal stresses in the crystal lattice will be determined by the expression [37]

$$\frac{\sigma}{\alpha} = \frac{0.27\ \text{nm}}{0.48\ \text{nm/GPa}} = 0.56\ \text{GPa}.$$

However, this method cannot specify directions of internal stresses in a crystal lattice because the dispersion of line positions cannot take negative values.

6. Conclusions

The present work describes the technology for synthesising high-quality ultra-nanosize diamonds, which comprise silica-vacancy colour centres. Nanodiamond dimensions have been found experimentally in two ways: by analysing AFM-maps (5.5 ± 5 nm) and TEM-images (7.5 ± 5 nm), which agrees with the values obtained by using the spatial phonon localisation theory (9.1 ± 1 nm). The crystal structure of synthesised nanodiamonds was investigated by using high-resolution TEM-images, X-Ray diffraction analysis of diamond material, and Raman spectroscopy. The upper limit of possible stresses was estimated (~0.56 GPa) from the dispersion of the phononless line position ($\sigma = 0.27$ nm). The line dispersion may be related to local stresses arising at crystalline aggregate boundaries. Thus, nanodiamonds synthesised by the method suggested are promising in quantum and biological applications due to small dimensions and high quality of the crystal structure.

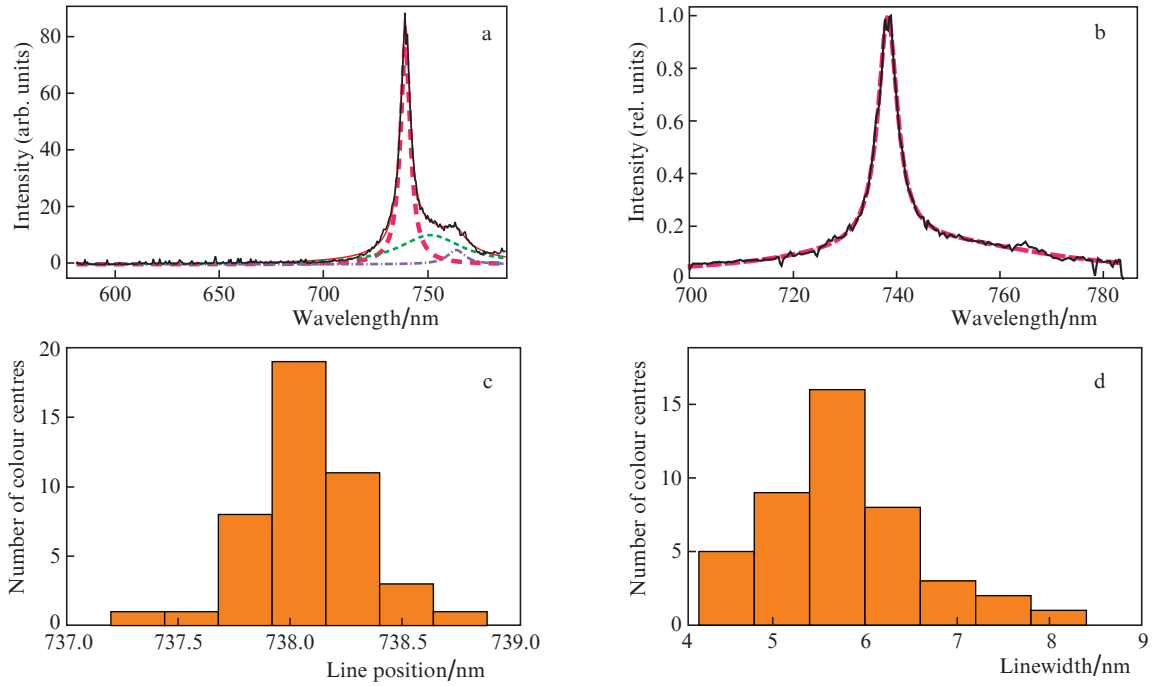

Figure 4. (Colour online) (a, b) Typical spectra (solid curves) of SiV-centre fluorescence at room temperature and their approximation by a sum of three Lorentz functions [dashed curves correspond to (a) phononless line and (b) approximation by the sum of three Lorentz functions, dashed and dotted curves refer to phonon wings) and (c, d) distribution histograms of the number of colour centres (c) over line centre position and (d) FWHM for the phononless line of SiV centres in various nanodiamonds.

Acknowledgements. The work was supported by the Russian Science Foundation (Grant No. 19-19-00693) and Russian Foundation for Basic Research (Grant No. 18-03-936).

References

1. Hui Y.Y., Cheng C.L., Chang H.C. *J. Phys. D: Appl. Phys*., **43**, 11 (2010).
2. Schrand A.M., Hens S.A.C., Shenderova O.A. *Crit. Rev. Solid State Mater. Sci*., **34**, 18 (2009).
3. Robledo L., Childress L., Bernien H., Hensen B., Alkemade P.F.A., Hanson R. *Nature*, **477**, 574 (2011).
4. Maurer P.C., Kucsko G., Latta C., Jiang L., Yao N.Y., Bennett S.D., Pastawski F., Hunger D., Chisholm N., Markham M., Twitchen D.J., Cirac J.I., Lukin M.D. *Science*, **336**, 1283 (2012).
5. Kharisov B.I., Kharissova O.V., Chávez-Guerrero L. *Synth. React. Inorg., Met. Nano-Metal Chem*., **40**, 84 (2010).
6. Vul A.Y., Shenderova O.A. *Detonation Nanodiamonds Science and Applications* (Stanford: Pan Stanford Publishing, 2013).
7. Ozawa M., Inaguma M., Takahashi M., Kataoka F., Krüger A., Osawa E. *Adv. Mater*., **19**, 1201 (2007).
8. Vlasov I.I., Barnard A.S., Ralchenko V.G., Lebedev O.I., Kanzyuba M.V., Saveliev A.V., Konov V.I., Goovaerts E. *Adv. Mater*., **21**, 808 (2009).
9. Ekimov E.A., Kudryavtsev O.S., Khomich A.A., Lebedev O.I., Dolenko T.A., Vlasov I.I. *Adv. Mater*., **27**, 5518 (2015).
10. Ekimov E.A., Kudryavtsev O.S., Mordvinova N.E., Lebedev O.I., Vlasov I.I. *ChemNanoMat*., **4**, 269 (2018).
11. Boudou J.P., Tisler J., Reuter R., Thorel A., Curmi P.A., Jelezko F., Wrachtrup J. *Diamond Relat. Mater*., **37**, 80 (2013).
12. Schirhagl R., Chang K., Loretz M., Degen C.L. *Annu. Rev. Phys. Chem*., **65**, 83 (2014).
13. Kurtsiefer C., Mayer S., Zarda P., Weinfurter H. *Phys. Rev. Lett*., **85**, 290 (2000).
14. Sildos I., Loot A., Kiisk V., Puust L., Hizhnyakov V., Yelisseyev A., Osvet A., Vlasov I. *Diamond Relat. Mater*., **76**, 27 (2017).
15. Iwasaki T., Ishibashi F., Miyamoto Y., Doi Y., Kobayashi S., Miyazaki T., Tahara K., Jahnke K.D., Rogers L.J., Naydenov B., Jelezko F., Yamasaki S., Nagamachi S., Inubushi T., Mizuochi N., Hatano M. *Sci. Rep*., **5**, 12882 (2015).
16. Aharonovich I., Castelletto S., Johnson B.C., McCallum J.C., Prawer S. *New J. Phys*., **13**, 045015 (2011).
17. Iwasaki T., Miyamoto Y., Taniguchi T., Siyushev P., Metsch M.H., Jelezko F., Hatano M. *Phys. Rev. Lett*., **119**, 253601 (2017).
18. Wang C., Kurtsiefer C., Weinfurter H., Burchard B. *J. Phys. B: At. Mol. Opt. Phys*., **39**, 37 (2006).
19. Bolshedvorskii S.V., Vorobyov V.V., Soshenko V.V., Shershulin V.A., Javadzade J., Zeleneev A.I., Komrakova S.A., Sorokin V.N., Belobrov P.I., Smolyaninov A.N., Akimov A.V. *Opt. Mater. Express*, **7**, 4038 (2017).
20. Sedov V., Ralchenko V., Khomich A.A., Vlasov I., Vul A., Savin S., Goryachev A., Konov V. *Diamond Relat. Mater*., **56**, 23 (2015).
21. Kalish R. *Diamond Relat. Mater*., **10**, 1749 (2001).
22. Häußler S., Thiering G., Dietrich A., Waasem N., Teraji T., Isoya J., Iwasaki T., Hatano M., Jelezko F., Gali A., Kubanek A. *New J. Phys*., **19**, 1 (2017).
23. Vlasov I.I., Shiryaev A.A., Rendler T., Steinert S., Lee S.Y., Antonov D., Vörös M., Jelezko F., Fisenko A.V., Semjonova L.F., Biskupek J., Kaiser U., Lebedev O.I., Sildos I., Hemmer P.R., Konov V.I., Gali A., Wrachtrup J. *Nat. Nanotechnol*., **9**, 54 (2014).
24. Bolshakov A., Ralchenko V., Sedov V., Khomich A.A., Vlasov I., Khomich A.V., Trofimov N., Krivobok V., Nikolaev S., Khmelnitskii R., Saraykin V. *Phys. Status Solidi A Appl. Mater. Sci*., **212**, 2525 (2015).
25. Davydov V.A., Rakhmanina A.V., Agafonov V., Narymbetov B., Boudou J.-P., Szwarc H. *Carbon*, **42**, 261 (2004).
26. Davydov V.A., Rakhmanina A.V., Lyapin S.G., Il'ichev I.D., Boldyrev K.N., Shiryaev A.A., Agafonov V.N. *JETP Lett*., **99**, 585 (2014) [*Pis'ma Zh. Exp. Teor. Fiz*., **99**, 613 (2014)].
27. Davydov V.A., Rakhmanina A.V., Agafonov V.N., Khabashesku V.N. *J. Phys. Chem. C*, **115**, 21000 (2011).
28. Bolshedvorskii S.V., Zeleneev A.I., Vorobyov V.V., Soshenko V.V., Rubinas O.R., Zhulikov L.A., Pivovarov P.A., Sorokin V.N., Smolyaninov A.N., Kulikova L.F., Garanina A.S., Lyapin S.G., Agafonov V.N., Uzbekov R.E., Davydov V.A., Akimov A.V. *ACS Appl. Nano Mater*., **2**, 4765 (2019).
29. Stehlik S., Varga M., Ledinsky M., Jirasek V., Artemenko A., Kozak H., Ondic L., Skakalova V., Argentero G., Pennycook T., Meyer J.C., Fejfar A., Kromka A., Rezek B. *J. Phys. Chem. C*, **119**, 27708 (2015).
30. Di Liscia E.J., Álvarez F., Burgos E., Halac E.B., Huck H., Reinoso M. *Mater. Sci. Appl*., **4**, 191 (2013).
31. Yoshikawa M., Mori Y., Maegawa M., Katagiri G., Ishida H., Ishitani A. *Appl. Phys. Lett*., **62**, 3114 (1993).
32. Ager J.W., Veirs D.K., Rosenblatt G.M. *Phys. Rev. B*, **43**, 6491 (1991).
33. Roy C., Hughes S. *Phys. Rev. X*, **1**, 1 (2011).
34. Jahnke K.D., Sipahigil A., Binder J.M., Doherty M.W., Metsch M., Rogers L.J., Manson N.B., Lukin M.D., Jelezko F. *New J. Phys*., **17**, 043011 (2015).
35. Nguyen C.T., Evans R.E., Sipahigil A., Bhaskar M.K., Sukachev D.D., Agafonov V.N., Davydov V.A., Kulikova L.F., Jelezko F., Lukin M.D. *Appl. Phys. Lett*., **112**, 203102 (2018).
36. Neu E., Steinmetz D., Riedrich-Möller J., Gsell S., Fischer M., Schreck M., Becher C. *New J. Phys*., **13**, 025012 (2011).
37. Lyapin S.G., Ilichev I.D., Novikov A.P., Davydov V.A., Agafonov V.N. *Nanosyst. Phys., Chem., Math*., **9**, 55 (2018).